z = transformed distance variable as defined by Equations (21), (22) or (23)

Greek Letters

θ = $k_1 t$

ϕ = enhancement factor, M_t/M_t^0

ϕ_A = maximum relative increase in diffusion rate

Subscripts

B = located in liquid bulk

I = absorption situation

II = desorption situation

Superscript

* = located at gas/liquid interface

LITERATURE CITED

1. Higbie R., *Trans. Am. Inst. Chem. Engr.*, **31**, 365 (1955).
2. Danckwerts, P. V., *Trans. Faraday Soc.*, **46**, 300 (1950).
3. Huang, Chen—Jung, and Chiang-Hai Kuo, *AIChE J.*, **11**, 901 (1965).
4. Toor, H. L., and S. H. Chiang, *ibid.*, **5**, 339 (1969).
5. Van Krevelyn, D. W., P. J. Hoftijzer, and F. J. Huntjens, *Rec. Trav. Chem. Pays-Bas Belg.*, **68**, 191 (1949).
6. Hatta, Shinoji, *Tohoku Imperial Univ. Tech. Rept.*, **10**, 119 (1932).
7. Cleander, D. R., *AIChE J.*, **5**, 339 (1959).
8. Crank, J., and P. Nicholson, *Proc. Cambridge Phil. Soc.*, **43**, 50 (1947).
9. Brian, P. L. T., J. F. Hurley, and E. H. Hasseltime, *AIChE J.*, **7**, 227 (1961).
10. Brian, P. L. T., J. E. Vivian, and A. G. Habib, *ibid.*, **8**, 205 (1962).
11. Brian, P. L. T., and M. C. Beaverstock, *Chem. Eng. Sci.*, **20**, 47 (1965).
12. Secor, R. M., and J. A. Beutler, *AIChE J.*, **13**, 365 (1967).
13. Richtmeyer, R. D., "Difference Methods for Initial Value Problems," Interscience, New York (1967).
14. Sherwood, T. K., and R. L. Pigford, "Absorption and extraction," 2nd edit., p. 328, McGraw-Hill, New York (1952).

Manuscript received June 3, 1969; revision received December 12, 1969; paper accepted December 19, 1969.

Convective Dispersion of Blood Gases in Curved Channel Exchangers

HSIN-KANG CHANG and LYLE F. MOCKROS

Northwestern University, Evanston, Illinois

The rates of hemoglobin saturation and carbon dioxide reduction in blood flowing in a curved channel membrane exchanger were studied theoretically by considering the fluid-limited process and the wall-limited process. The fluid-limited process was studied for laminar flows with and without secondary circulations. The relatively nontraumatic centrifugally induced circulations in the curved channel can reduce the required channel length to less than 1/500 that required for unperturbed flow. Such improvement, however, is practical only if very permeable membranes are available. If the P_{O_2} = 715 mm. Hg and P_{CO_2} = 0 mm. Hg at the walls, the fluid-limited analyses show oxygenation to be the slower process and the wall-limited analyses indicate CO_2 removal to be the limiting process. If the best available silicone rubber membranes are used, the process will be fluid limited for the unperturbed flow and wall limited for the flow with secondary circulations.

The use of auxiliary respiratory gas exchangers to restore venous blood to arterial conditions is commonplace today in cardiac surgical procedures. Nevertheless, the need remains for better designed exchangers, and much of the current interest centers on development of membrane exchangers. Recent analyses have described the characteristics of membrane exchangers consisting of straight tubes (*23, 2*), coiled tubes (*24, 6*), oscillating coiled tubes (*8*), annuli with stationary walls (*4*), annuli with an outer moving wall (*12*), and a rectangular channel with one moving wall (*22*). With the presently available membranes and with reasonable sizes, the analyses indicate that the process is limited by the gas transfer in the fluid phase

Hsin-kang Chang is at the State University of New York, Buffalo, New York.

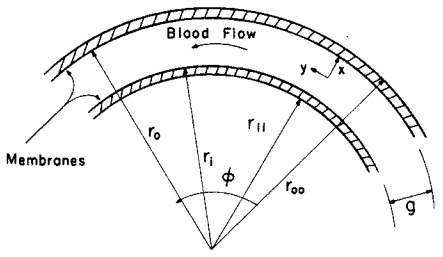

Fig. 1. Geometry and notation for curved channel.

unless some transverse mixing is induced. A relatively gentle (imperative in any blood handling) and effective method of mixing is to induce secondary circulations. The present paper considers the gas transfer to and from blood flowing in a curved channel. The flow is assumed to be driven by a pressure gradient. Parallel laminar flow in curved channels exhibits centrifugal instability for critical conditions. The instability induces a second laminar mode with a secondary circulation in the form of cellular vortices (3). These vortices can greatly enhance the gas transfer in the fluid phase and thereby greatly improve the overall efficiency.

If the gap width, as shown in Figure 1, is small compared with the mean radius; that is

$$g = r_o - r_i << \frac{1}{2}(r_i + r_o) = r_m \qquad (1)$$

the channel may be considered as the space between parallel planes and the unperturbed flow may be described by the velocity distribution for plane Poiseuille flow. Throughout this analysis, the condition given by Equation (1) is assumed to hold.

For both ease of analysis and ease of presentation, the gas transfer process is studied by investigating two limiting cases: the fluid-limited case and the wall-limited case. The fluid-limited analysis assumes that the membrane is infinitely permeable to the gases and involves the solution of nonlinear convective diffusion equations. The wall-limited analysis assumes that the mixing is instantaneous and only requires the solution of the steady state diffusion equation for the wall. In the fluid-limited case the convective diffusion equation contains a term representing the source-sink characteristics for the respiratory gases in blood. Derived from dissociation curves (23), the term may be approximated by an exponential function

$$f(C) = 234 \exp(-2.57 \times 10^4\, C) + 40.6 \exp(-2.25 \times 10^4\, C + 1.14) \qquad (2)$$

for the case of oxygenation and a constant

$$f(C) = 9.0 \qquad (3)$$

for the case of carbon dioxide removal. The $f(C)$ for oxygenation is an accurate curve fit; the $f(C)$ for carbon dioxide is only a linearization of the absorption curve and as such is a first-order approximation.

FLUID-LIMITED ANALYSIS: UNPERTURBED LAMINAR FLOW

Oxygenation

In Cartesian coordinates the plane Poiseuille velocity distribution is

$$V_y(x) = \frac{3}{2} V_m \left[1 - 4\left(\frac{x}{g}\right)^2\right] \qquad (4)$$

in which $V_m = -(g^2/12\mu)(dp/dy)$ is the mean velocity.

Defining the dimensionless variables

$$x^* = \frac{x}{g};\quad y^* = \frac{D}{V_m g^2} y;\quad V_y^* = \frac{V_y}{V_m} \qquad (5)$$

one may write the gas transport equation (23, 19, 4) in Cartesian coordinates:

$$[1 + f(C)]\, V_y^* \frac{\partial C}{\partial y^*} = \frac{\partial^2 C}{\partial x^{*2}} + \left(\frac{D}{V_m g}\right)^2 \frac{\partial^2 C}{\partial y^{*2}} \qquad (6)$$

The last term in Equation (6) represents tangential diffusion and is a product of two small quantities in comparison with the other terms, so the equation solved is

$$[1 + f(C)]\, \frac{3}{2}(1 - 4x^{*2}) \frac{\partial C}{\partial y^*} = \frac{\partial^2 C}{\partial x^{*2}} \qquad (7)$$

The boundary conditions are

$$C(x^*, 0) = C_e \qquad (8)$$

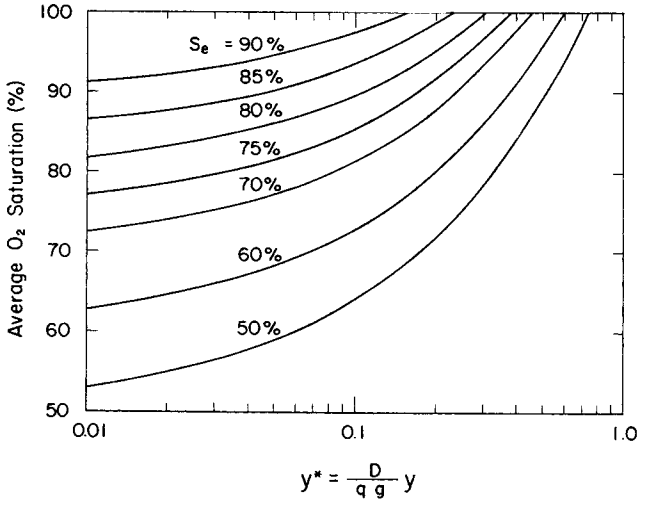

Fig. 2. Average oxygen saturation of sample exiting channel exchanger as a function of dimensionless channel length and parametrically as a function of entrance saturation. The flow is assumed to be unperturbed laminar flow and the exchange process is assumed to be fluid limited. Hemoglobin concentration is 15 g.%. The wall P_{O_2} is 715 mm. Hg.

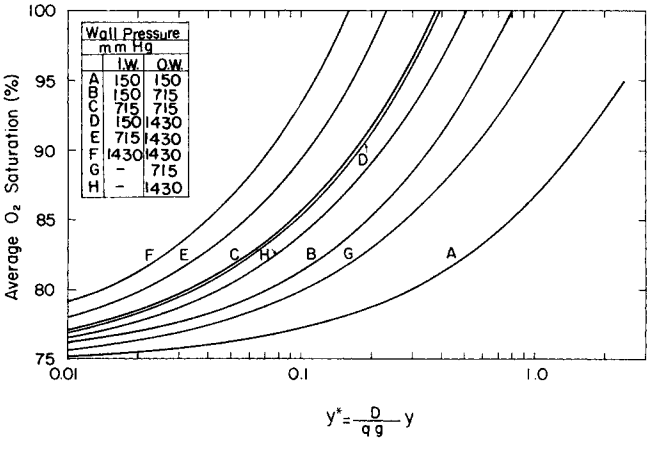

Fig. 3. Average oxygen saturation of sample exiting channel exchanger as a function of dimensionless channel length and parametrically as a function of the wall P_{O_2}. The flow is assumed to be unperturbed laminar flow and the exchange process is assumed to be fluid limited. The hemoglobin concentration is 15 g.% and the entrance saturation is 75%.

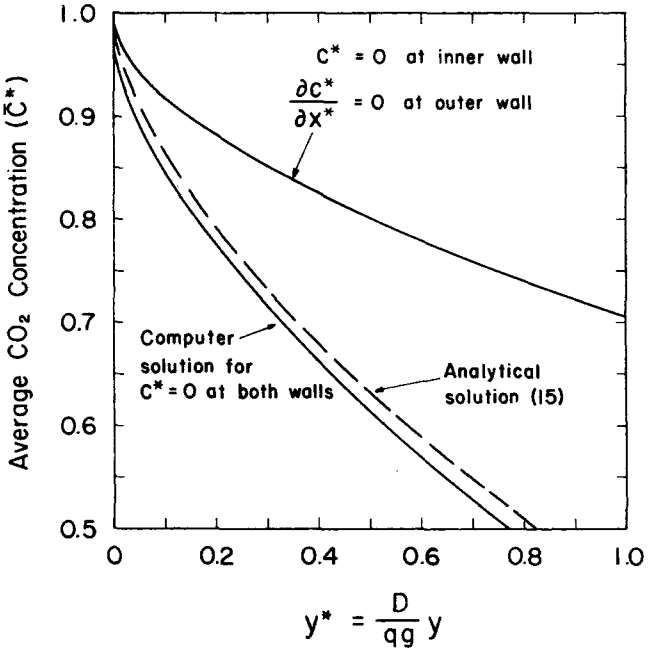

Fig. 4. Average carbon dioxide concentration of sample exiting channel exchanger as a function of dimensionless channel length and parametrically as a function of wall conditions. Broken line is adapted from analytical solution for heat transfer problem (14). Flow is assumed to be unperturbed laminar flow and the exchange process is assumed to be fluid limited.

$$C\left(-\frac{1}{2}, y^*\right) = C_i; \quad y > 0 \tag{9}$$

and

$$C\left(\frac{1}{2}, y^*\right) = C_o; \quad y > 0 \tag{10}$$

The system defined by Equations (7) and (10) was solved numerically with an explicit finite-difference method.

Since the term involving D/V_mg is omitted, the solution of Equation (7) is independent of this parameter. A parametric study of this problem was made by varying the initial oxygen saturation conditions in the blood and the boundary values. The results of various entrance saturations with the oxygen pressure at both walls held at 715 mm. Hg are shown in Figure 2. The curves in Figure 3 are the solutions obtained, with a 75% entrance saturation, for various oxygen pressures at the walls. The ordinates on Figure 2 and Figure 3 are the oxygen saturation of a cup-mixed sample exiting the exchanger.

Carbon Dioxide Removal

The dimensionless equation for carbon dioxide removal is

$$10\, V_y^* \frac{\partial C^*}{\partial y^*} = \frac{\partial^2 C^*}{\partial x^{*2}} + \left(\frac{D}{V_m g}\right)^2 \frac{\partial^2 C^*}{\partial y^{*2}} \tag{11}$$

where x^*, y^*, and V^* are defined in Equation (5) and

$$C^* = \frac{C - C_i}{C_e - C_i} \tag{12}$$

As in the previous case, the longitudinal diffusion term can be neglected. Thus

$$15\,(1 - 4x^{*2}) \frac{\partial C^*}{\partial y^*} = \frac{\partial^2 C^*}{\partial x^{*2}} \tag{13}$$

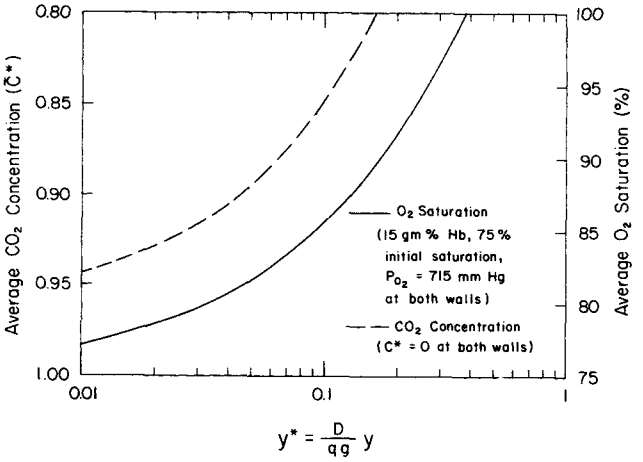

Fig. 5. Comparison of fluid-limited oxygen uptake and carbon dioxide removal for laminar unperturbed flow in channel exchanger.

was solved with the following boundary conditions:

$$C^*(x^*, 0) = 1 \tag{14}$$

$$C^*\left(-\frac{1}{2}, y^*\right) = 0 \tag{15}$$

$$C^*\left(\frac{1}{2}, y^*\right) = \frac{C_o - C_i}{C_e - C_i} \tag{16}$$

Numerical solutions were obtained for two cases: both walls with zero carbon dioxide concentration, that is, $C_o = C_i = 0$; and inner wall (or lower plate) with zero concentration and outer wall (or upper plate) impermeable, that is, $C_i = 0$, $\left.\frac{\partial C}{\partial x^*}\right|_o = 0$. The results are plotted in Figure 4.

An analytical solution of the first case has been obtained by Prins et al. (*14*) in a heat transfer problem. When the necessary transformations are made, their solution, in terms of average dimensionless concentration, is:

$$C^* = 0.914\, e^{-0.754y^*} + 0.053\, e^{-8.59y^*} + 0.015\, e^{-24.92y^*} + \ldots \tag{17}$$

This analytical solution is represented in Figure 4 by the broken line. The discrepancy between the analytical and computer solutions is perhaps the result of both inaccurate computation on the part of Prins et al. and the discretization errors which tend to be on the optimistic side.

Figure 5 indicates, since $D_{O_2} \approx D_{CO_2}$, that with these wall conditions and a homeostatic range for oxygen and carbon dioxide concentrations, oxygenation is the limiting factor in the laminar tangential flow case. In order to prevent overelimination of carbon dioxide, some carbon dioxide partial pressure should be provided at the walls or, alternatively, a higher P_{O_2} should be used at the walls.

Although the primary purpose of this study is to analyze the blood flow in a curved channel, this solution is obviously applicable to the case of blood flow between two flat sheets of permeable material, such as used in the early Clowes-type membrane oxygenators (*9*).

FLUID-LIMITED ANALYSIS: FLOW WITH SECONDARY CIRCULATION

The stability of fluid flow along a two-dimensional curved channel under the action of a pressure gradient was first examined by Dean (5). When the curved chan-

nel is contained within two concentric cylinders, he found that the motion becomes unstable when the Dean number, $N_D = N_{Re}\,(g/r_i)^{1/2}$, exceeds a value of about 36; g is the spacing between the walls, assumed small compared with r_i, the radius of the inner wall; and $N_{Re} = V_m g/\nu$ is Reynolds number based on the mean velocity V_m of the unperturbed flow. A secondary cellular pattern of motion ensues that is not unlike Taylor vortices. Using different methods, Reid (*15*) and Hammerlin (*11*) arrived at similar conclusions. Brewster et al. (*1*) performed experiments by pumping glycerine solutions of varying viscosity between two horizontal, concentric cylinders and found experimental values in good agreement with the theoretical values. The induced vortices can be expected to greatly enhance mass convection in the fluid system. In heat transfer Gazley (*10*) reported a higher heat transfer rate in the presence of Taylor vortices than with turbulent flow.

Using a dimensionless, pseudorectilinear coordinate (see Figure 1)

$$x^* = \frac{r - r_i}{r_o - r_i} - \frac{1}{2} \tag{18}$$

the velocity distribution of the unperturbed flow is

$$V_y(x^*) = \frac{3}{2} V_m\,(1 - 4x^{*2}) \tag{19}$$

in which

$$V_m = -\frac{g^2}{12\mu\, r_m}\,\frac{\partial p}{\partial \varphi}$$

The disturbance takes the form of vortices periodic in the z direction and symmetric with respect to φ. Figure 6 shows the streamlines for such vortices in an arbitrary meridian plane. Based on a linear analysis, Reid (*15*) obtained the shape of the velocity components of the disturbance. If

$$y^* = \frac{y}{g} \quad \text{and} \quad z^* = \frac{z}{g} \tag{20}$$

are defined as the dimensionless coordinates in the tangential and axial directions, respectively, and an amplitude factor is added, Reid's results may be written as follows:

$$v_x = -\frac{\alpha a}{g}\,\psi\,(x^*)\cos\,(az^*) \tag{21}$$

$$v_y = -\frac{6\,N_{Re}\,\alpha a}{g}\,\gamma\,(x^*)\cos\,(az^*) \tag{22}$$

and

$$v_z = \frac{\alpha\,\psi\,(x^*)\sin\,(az^*)}{r_m + x^*\,g} + \frac{\alpha}{g}\,\psi'\,(x^*)\sin\,(az^*) \tag{23}$$

In the above equations, α, having a dimension of L^2/T, is the amplitude factor, $a = 3.98$ is the dimensionless critical wave number of the disturbance

$$\psi(x^*) = \sum_{m=1}^{\infty} [A_m\,C_m\,(x^*) + B_m\,S_m\,(x^*)] \tag{24}$$

is the dimensionless stream function, and

$$\gamma(x^*) = \sum_{m=1}^{\infty} A_m \left\{ a_m \frac{\sinh\,(ax^*)}{\sinh\,(\tfrac{1}{2}\,a)} - \frac{2x^*}{\lambda_m{}^4 - a^4}\,[a^2\,C_m\,(x^*) + C_m''\,(x^*)] + \frac{4}{(\lambda_m{}^4 - a^4)^2}\,[(\lambda_m{}^4 + a^4)\,C_m'\,(x^*) + 2a^2\,C'''\,(x^*)] \right\}$$
$$+ \sum_{m=1}^{\infty} B_m \left\{ b_m \frac{\cosh\,(ax^*)}{\cosh\,(\tfrac{1}{2}\,a)} - \frac{2x^*}{\mu_m{}^4 - a^4}\,[a^2\,S_m\,(x^*) + S_m''\,(x^*)] + \frac{4}{(\mu_m{}^4 - a^4)^2}\,[(\mu_m{}^4 + a^4)\,S_m'\,(x^*) + 2a^2\,S_m'''\,(x^*)] \right\} \tag{25}$$

gives the radial variation of the tangential velocity of the disturbance. In Equations (24) and (25), A_m, B_m, λ_m, μ_m are coefficients and

$$C_m(x^*) = \frac{\cosh\,(\lambda_m\,x^*)}{\cosh\,(\tfrac{1}{2}\,\lambda_m)} - \frac{\cos\,(\lambda_m\,x^*)}{\cos\,(\tfrac{1}{2}\,\lambda_m)} \tag{26}$$

$$S_m(x^*) = \frac{\sinh\,(\mu_m\,x^*)}{\sinh\,(\tfrac{1}{2}\,\mu_m)} - \frac{\sin\,(\mu_m\,x^*)}{\sin\,(\tfrac{1}{2}\,\mu_m)} \tag{27}$$

$$a_m = \frac{2\lambda_m{}^2}{\lambda_m{}^4 - a^4} - \frac{16a^2\,\lambda_m{}^3\tanh\,(\tfrac{1}{2}\,\lambda_m)}{(\mu_m{}^4 - a^4)^2} \tag{28}$$

and

$$b_m = \frac{2\mu_m{}^2}{\mu_m{}^4 - a^4} - \frac{16a^2\,\mu_m{}^3\coth\,(\tfrac{1}{2}\,\mu_m)}{(\mu_m{}^4 - a^4)^2} \tag{29}$$

The first-order coefficients have been calculated by Reid, and are

$$A_1 = 1.0, \quad B_1 = 0.2719, \quad \lambda_1 = 4.7300407449,$$
$$\mu_1 = 7.8532046241 \tag{30}$$

The amplitude factor α cannot be determined from the linear analysis. In a paper treating the nonlinear mechanics of hydrodynamic stability, Stuart (*20*) showed that for Couette flow

$$\alpha = \frac{\beta}{N_{Re}}\left(1 - \frac{T_c}{T}\right)^{1/2} \tag{31}$$

in which β is a constant

$$T = N_{Re}{}^2\,\frac{g}{r_i} \tag{32}$$

is the Taylor number, and T_c is the critical Taylor number. Calculations based on Stuart's analysis indicate that for the Couette flow with a Taylor number 5% greater than the critical Taylor number, the average disturbance velocity has a magnitude that is 3.7% as large as the average velocity of the main flow. A similar nonlinear analysis is not available for the pressure-driven flow of the present study, and the above analysis for the Couette case was

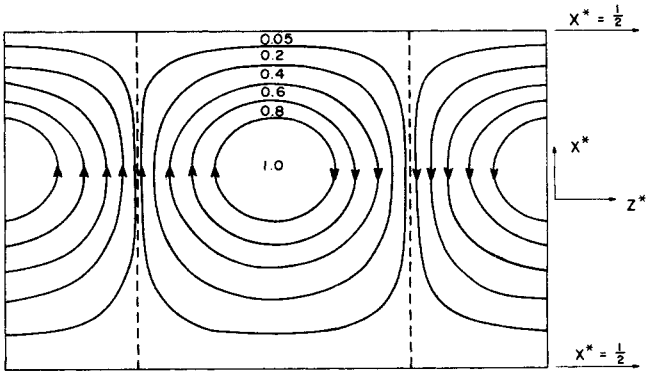

Fig. 6. Normalized stream function for perturbed cellular motion in curved channel.

used to estimate the strength of the secondary flow. Thus for the present case, T_c = (critical Dean number)^2 = 36^2, and if the constant β is chosen as 50, that is

$$\alpha = \frac{50}{N_{Re}} \left(1 - \frac{T_c}{T}\right)^{1/2} \tag{33}$$

the resulting secondary flows are about the proper strength. For example, if the ratio g/r_i is 0.1 at $T = (N_D)^2 = 5\%$ higher than the critical number, α is 0.093, giving an average disturbance velocity of about 4.3% of V_m. The sensitivity of the resulting gas transport to the choice of β was tested by using two other estimates of β, one larger than 50 and one smaller than 50. These results are discussed below.

Combining the main flow and the first-order approximation of the disturbance, one can describe the velocity field of the equilibrium flow by

$$V_x = v_x = -\frac{\alpha a}{g} [C_1(x^*) + 0.2719\, S_1(x^*)] \cos(az^*) \tag{34}$$

$$V_y = V(x^*) + v_y$$

$$= \frac{3}{2} V_m (1 - 4x^{*2}) - \frac{6\alpha a N_{Re}}{g} \gamma(x^*) \cos(az^*) \tag{35}$$

$$V_z = v_z$$

$$= \frac{\alpha}{r_m + x^*\, g} [C_1(x^*) + 0.2719\, S_1(x^*)] \sin(az^*)$$

$$+ \frac{\alpha}{g} [C_1'(x^*) + 0.2719\, S_1'(x^*)] \sin(az^*) \tag{36}$$

in which

$$\gamma(x^*)$$

$$= \left[\frac{2\lambda_1^2}{\lambda_1^4 - a^4} - \frac{16 a^2 \lambda_1^3 \tanh(\frac{1}{2}\lambda_1)}{(\lambda_1^4 - a^4)^2}\right] \frac{\sinh(ax^*)}{\sinh(\frac{1}{2}a)}$$

$$- \frac{2x^*}{\lambda_1^4 - a^4} [a^2 C_1(x^*) + C_1''(x^*)]$$

$$+ \frac{4}{(\lambda_1^4 - a^4)^2} (\lambda_1^4 + a^4) [C_1'(x^*) + 2a^2 C_1'''(x^*)]$$

$$+ 0.2719 \left\{ \left[\frac{2\mu_1^2}{\mu_1^4 - a^4} - \frac{16 a^2 \mu_1^3 \coth(\frac{1}{2}\mu_1)}{(\mu_1^4 - a^4)^2}\right] \right.$$

$$\frac{\cosh(ax^*)}{\cosh(\frac{1}{2}a)} - \frac{2x^*}{\mu_1^4 - a^4} [a^2 S_1(x^*) + S_1''(x^*)]$$

$$\left. + \frac{4}{(\mu_1^4 - a^4)^2} [(\mu_1^4 + a^4) S_1'(x^*) + 2a^2 S_1'''(x^*)] \right\} \tag{37}$$

$C_1(x^*)$, $S_1(x^*)$, and λ_1 and μ_1 are defined in Equations (26), (27), and (30), respectively.

The velocity components vanish at the boundaries of the cylinders, that is

$$V_x = V_y = V_z = 0, \quad \text{at} \quad x = \pm\frac{1}{2} \tag{38}$$

Oxygenation

Written in Cartesian coordinates, the dimensionless equation for the oxygenation during equilibrium flow is

$$\frac{\partial^2 C}{\partial x^{*2}} + \frac{\partial^2 C}{\partial y^{*2}} + \frac{\partial^2 C}{\partial z^{*2}} = [1 + f(C)]$$

$$\left[V_x^* \frac{\partial C}{\partial x^*} + V_y^* \frac{\partial C}{\partial y^*} + V_z^* \frac{\partial C}{\partial z^*} \right] \tag{39}$$

in which

$$V_x^* = -\xi a \cos(az^*) [C_1(x^*) + 0.2719\, S_1(x^*)] \tag{40}$$

$$V_y^* = 1.5\, N_{Re}\, N_{Sc} (1 - 4x^{*2})$$

$$- 6\, \xi a\, N_{Re} \cos(az^*)\, \gamma(x^*) \tag{41}$$

$$V_z^* = \xi \sin(az^*)$$

$$\left[\frac{1}{r_m^* + x^*} [C_1(x^*) + 0.2719\, S_1(x^*)] \right.$$

$$\left. + C_1'(x^*) + 0.2719\, S_1'(x^*) \right] \tag{42}$$

are the dimensionless velocity components. Furthermore

$$r_m^* = r_m/g \tag{43}$$

$$N_{Re} = V_m\, g/\nu \tag{44}$$

$$N_{Sc} = \nu/D \tag{45}$$

$$\xi = \frac{\alpha}{D} = \frac{\beta}{D\, N_{Re}} \left(1 - \frac{T_c}{T}\right)^{1/2}$$

$$= \frac{50}{D\, N_{Re}} \left[1 - \frac{1296 (r_m^* - 0.5)}{N_{Re}^2}\right]^{1/2} \tag{46}$$

Since the main flow is in the tangential (y^*) direction and diffusion is dominantly normal to that direction, the tangential diffusion term, in Equation (39), is of little importance and can be omitted. The remaining equation

$$\frac{\partial^2 C}{\partial x^{*2}} + \frac{\partial^2 C}{\partial z^{*2}}$$

$$= [1 + f(C)] \left[V_x^* \frac{\partial C}{\partial x^*} + V_y^* \frac{\partial C}{\partial y^*} + V_z^* \frac{\partial C}{\partial z^*} \right] \tag{47}$$

is parabolic and can be solved numerically for a set of appropriate boundary values.

Since the equilibrium flow is periodic along the axial (z^*) direction, and since within each period there are two cellular vortices differing from each other only in the sense of rotation, the gas transport problem in the annulus can be studied by considering the domain of one single cell. Thus the boundary conditions are

$$C(x^*, 0, z^*) = C_e; \qquad -\frac{1}{2} < x^* < \frac{1}{2},$$

$$0 < z^* < \frac{\pi}{a} \tag{48}$$

$$C\left(-\frac{1}{2}, y^*, z^*\right) = C_i; \quad y^* \geq 0 \tag{49}$$

$$C\left(\frac{1}{2}, y^*, z^*\right) = C_o; \qquad y^* \geq 0 \tag{50}$$

and

$$\frac{\partial C}{\partial z^*}(x^*, y^*, 0) = \frac{\partial C}{\partial z^*}\left(x^*, y^*, \frac{\pi}{a}\right) = 0 \tag{51}$$

A finite-difference method was employed to solve the system defined by Equations (47) to (51). Details of the

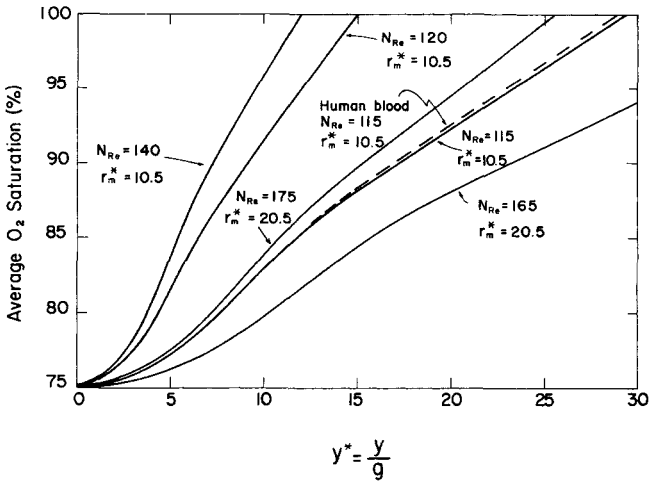

Fig. 7. Average oxygen saturation in sample exiting channel exchanger as a function of channel length and parametrically as a function of Reynolds number and dimensionless mean radius. The flow is assumed to be the perturbed laminar flow with secondary circulations and the exchange process is assumed to be fluid limited. The hemoglobin concentration is 15 g.%, the entrance saturation is 75%, and the wall P_{O_2} is 715 mm. Hg. The Schmidt number is 4,000.

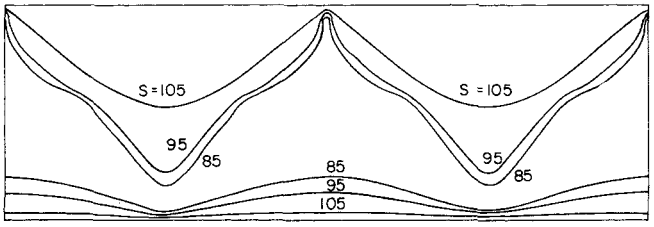

Fig. 8. Isosaturation lines in meridian plane for perturbed laminar flow in curved channel exchanger. The exchange process is assumed to be fluid limited, and the wall P_{O_2} is 715 mm. Hg. The hemoglobin concentration is 15 g.% and the entrance saturation is 75%. The cup-mixed average saturation is 90%.

numerical solution are given in the Appendix.† A special feature of the numerical method is the selective use of forward and backward differences for the radial and axial convective terms. Backward differences are used with positive velocities and forward differences with negative velocities. This technique makes the elements of the solution matrix satisfy the condition given by Saul'yev (*18*) for a unique solution.

Besides the three boundary values, four parameters are involved in the solution of Equation (47). These parameters are defined in Equations (43) to (46), respectively. The dimensionless mean radius r_m^*, representing the curvature, dictates the critical Reynolds number at which the vortices first appear. As the Reynolds number increases beyond the critical value, the strength of the secondary circulation increases and so does the expected enhancement of the rate of oxygenation. When the values of r_m^* and N_{Re} are known, the amplitude factor α is determined since β takes on an assumed value. Throughout this analysis $\beta = 50$, except when the specific effect of β is studied. The Schmidt number, the other parameter, also plays an important role in the mass transfer.

† The appendix has been deposited as document 01321 with the ASIS National Auxiliary Publications Service, c/o CCM Information Sciences, Inc., 909 Third Ave., New York 10022 and may be obtained for $2.00 for microfiche or $6.50 for photocopies.

Since the condition for the appearance of the vortices is

$$N_{Re}\,(g/r_i)^{1/2} > 36 \qquad (52)$$

a dimensionless mean radius of 10.5, that is, $g/r_i = 0.1$, requires that the Reynolds number be greater than 114. At a Reynolds number of 115, the average velocity of the secondary circulation is 2.87% of that of the unperturbed main flow. A milder curvature, for example, $r_m^* = 20.5$, requires a higher critical Reynolds number ($N_{Re} = 161$), and when $N_{Re} = 165$ the secondary velocity is 2.14% of the main flow velocity. Solutions obtained for both of these cases are shown in Figure 7. Note that although the latter case has a slightly stronger secondary circulation (mean velocity is directly proportional to the Reynolds number and $165 \times 2.14\% > 115 \times 2.87\%$), it is less efficient in oxygenation. The average residence time of a red cell in the oxygenator is much shorter in the latter case. Other values of r_m^* were not tried because a significantly smaller r_m^* would probably have invalidated the small gap assumption [Brewster et al. (*1*) used $r_m^* = 12.5$ in their experiments] and a significantly greater value would have required too high a critical velocity. If a pair of cylinders with a mean radius of 10.5 cm. and gap width of 1.0 cm. is used and a mean velocity of 4.6 cm./sec. is maintained ($R_{Re} = 115$), 25% saturation increase can be achieved in a distance of 30 cm. Compared with those obtained without the secondary circulation, this represents an improvement of 580-fold, provided, of course, that the process is still fluid limited.

Also shown in Figure 7 are the variations of solution with the Reynolds number, when the dimensionless mean radii are 10.5 and 20.5, respectively. A higher Reynolds number, hence a stronger secondary circulation, yields a higher oxygenation rate.

The broken line in Figure 7 represents the solution for human blood, while all other solutions were obtained for cattle blood. Its proximity to the cattle blood solution demonstrates that the dissociation curve assumed has little effect on the overall oxygenation process.

Isosaturation lines for an average saturation of 90% are plotted in Figure 8. The effect of the secondary circulation clearly can be seen from the spreading of the contour lines. Since the vortex strength is weaker in the lower half, the lines in the lower half do not move as far as those in the upper half.

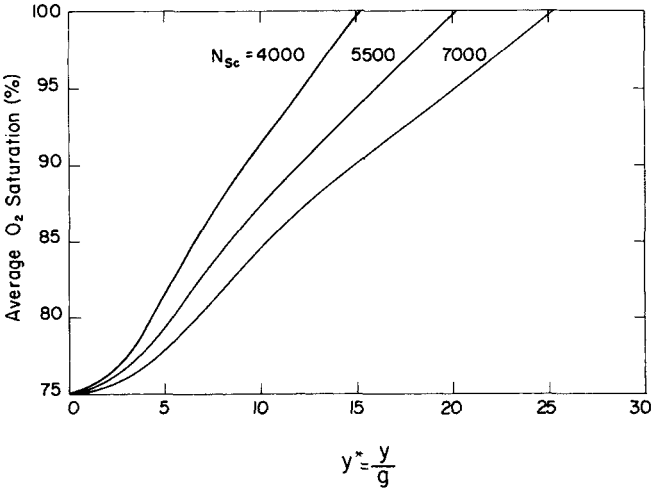

Fig. 9. Parametric variation of fluid-limited oxygenation process with Schmidt number for perturbed laminar flow in channel exchanger. The dimensionless mean radius is 10.5, the Reynolds number is 120, the entrance saturation is 75%, and the wall P_{O_2} is 715 mm. Hg.

An increase of Schmidt number means either an increased viscosity or decreased diffusivity, both of which have an adverse effect on mass transport as is evidenced in Figure 9.

An investigation on the effects of oxygen pressure variation at the walls is illustrated in Figure 10. Comparison of this figure with Figure 3 indicates that the effect of increased oxygen pressure at the walls is less pronounced in the present case than in the case where molecular diffusion is the only mechanism of oxygen transport. In the present case, as long as the pressure gradient between the wall and the blood adjacent to it is steep enough to maintain an ample supply of oxygen into the blood, the rate of oxygen saturation depends largely on the rate of convection, which transports the oxygen to the interior. Excess oxygen near the boundary has little effect in bringing up the average saturation.

The amplitude factor α is directly proportional to the constant β, which has been assumed to be 50. When the Reynolds number is 115 and Schmidt number is 4,000, the secondary circulation given by $\beta = 50$ is 2.87% of the main flow. If $\beta = 15$ and $\beta = 85$ are assumed, the secondary flow is 0.86% and 4.89%, respectively, of the main flow. Oxygenation rates of these three cases are shown in Figure 11.

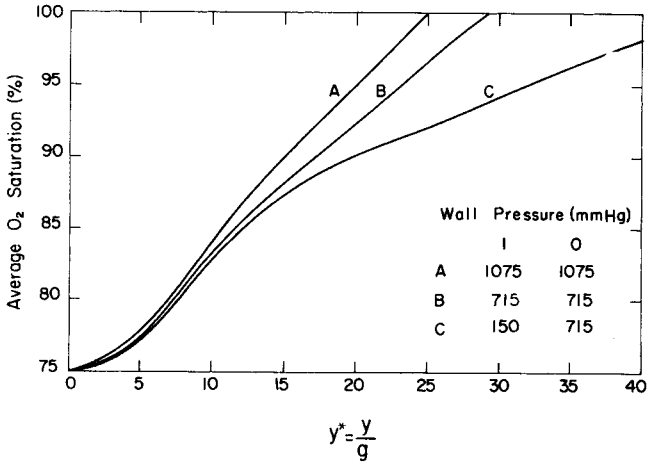

Fig. 10. Saturation increase for various wall conditions with perturbed flow in channel exchanger. The dimensionless mean radius is 10.5, the Reynolds number is 115, the Schmidt number is 4,000, and the entrance saturation is 75%.

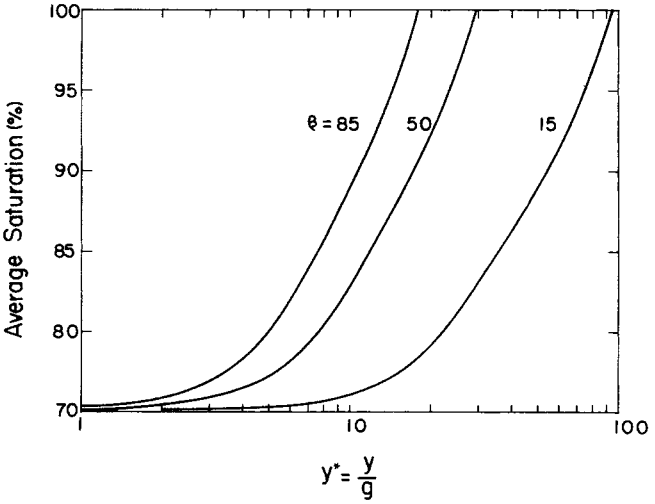

Fig. 11. Average oxygen saturation in sample exiting channel exchanger as a function of channel length and parametrically as a function of secondary circulation strength. The process is assumed to be fluid limited. The dimensionless mean radius is 10.5, the Reynolds number is 115, the Schmidt number is 4000, the entrance saturation is 75%, and the wall P_{O_2} is 715 mm. Hg.

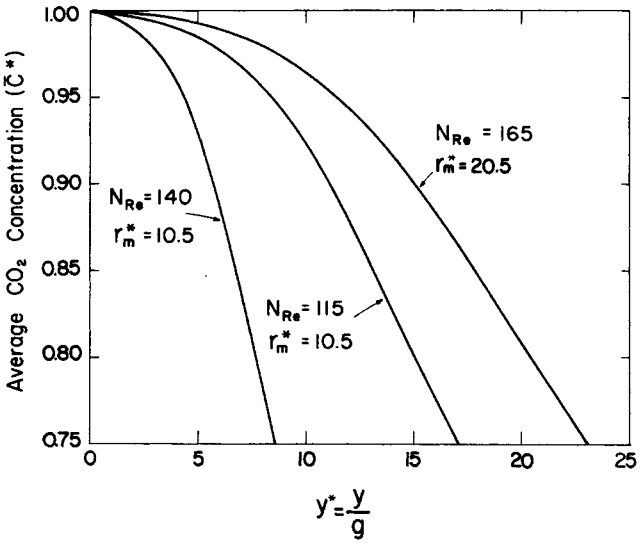

Fig. 12. Average carbon dioxide saturation in sample exiting channel exchanger as a function of channel length and parametrically as a function of Reynolds number and dimensionless mean radius. The flow is assumed to be the perturbed laminar flow with secondary circulations and the exchange process is assumed to be fluid limited. The Schmidt number is 4,000, the entrance concentration is 1.0, and the wall concentration is zero.

Carbon Dioxide Removal

The governing equation for the carbon dioxide removal is

$$\frac{\partial^2 C^*}{\partial x^{*2}} + \frac{\partial^2 C^*}{\partial z^{*2}} = 10 \left[V_x^* \frac{\partial C^*}{\partial x^*} + V_y^* \frac{\partial C^*}{\partial y^*} + V_z^* \frac{\partial C^*}{\partial z^*} \right] \quad (53)$$

in which

$$C^* = \frac{C - C_i}{C_e - C_i} \quad (54)$$

The dimensionless boundary conditions are

$$C^*(x^*, y^*, 0) = 1 \quad (55)$$

$$C^*\left(-\frac{1}{2}, y^*, z^*\right) = 0 \quad (56)$$

$$C^*\left(\frac{1}{2}, y^*, z^*\right) = \frac{C_o - C_i}{C_e - C_i} = 0 \text{ if } C_o = C_i \quad (57)$$

and

$$\frac{\partial C^*}{\partial z^*}(x^*, y^*, 0) = \frac{\partial C^*}{\partial z^*}\left(x^*, y^*, \frac{\pi}{a}\right) = 0 \quad (58)$$

The above system was solved numerically on a digital computer and details of the numerical solution are given in the Appendix. Figure 12 shows the difference in carbon dioxide removal rate when the dimensionless mean radius is varied. As might be expected, increasing the Reynolds number speeds up the carbon dioxide removal. Results of varying the Schmidt number are shown in Figure 13. The concentration profile for $\bar{C}^* = 0.855$ is shown in Figure 14.

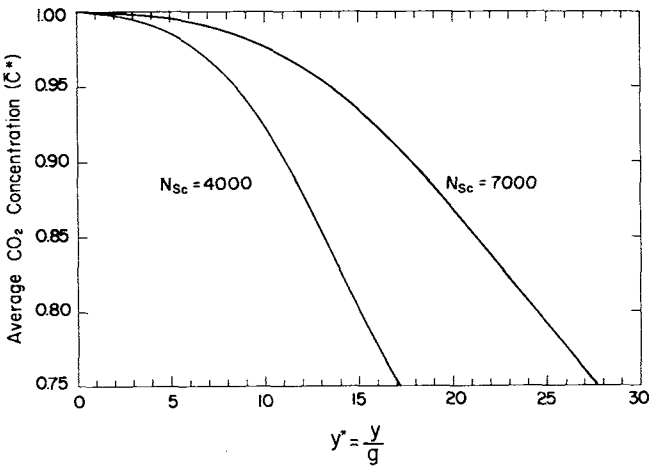

Fig. 13. Parametric variation of fluid-limited carbon dioxide removal process with Schmidt number for perturbed flow in channel exchanger. The dimensionless mean radius is 10.5, the Reynolds number is 115, and the entrance concentration is 1.0.

Summary

Corresponding solutions for oxygenation and carbon dioxide removal may be compared. As concluded in the previous section, oxygenation is the limiting factor, as long as these wall conditions are used. In order to prevent over-elimination of carbon dioxide, the dimensionless carbon dioxide concentration corresponding to the length required for complete hemoglobin saturation should be found and then the carbon dioxide partial pressure needed at the walls may be computed by

$$C^* = \frac{40 - (P_{CO_2})_w}{47 - (P_{CO_2})_w} \tag{59}$$

The results of this analysis indicate that the fluid system is very efficient in achieving the desired oxygen saturation and carbon dioxide elimination. Whether a practical oxygenator can be constructed to have the calculated efficiency depends on the permeability of the wall.

WALL-LIMITED ANALYSIS

The rate of gas diffusion through the annular walls has been determined in a previous paper already cited (*4*). Since the fluid-limited analyses above were carried out in Cartesian coordinates, it is convenient to consider the wall-limited analysis in the same coordinates.

Derived from Fick's law the mass flux (per unit width) through two parallel membranes can be shown to be

$$F = L\,(DK)_w \left(\frac{P_{ii} - P_i}{T_i} + \frac{P_{oo} - P_o}{T_o} \right) M/(\text{min.})\,(\text{cm.}) \tag{60}$$

where L is the length of the plates, $(DK)_w$ is the wall permeability and T_i and T_o are the thicknesses of the inner and outer membranes, respectively. The letter P denotes partial pressure and the subscripts have the same meaning as those in Figure 1. When the annular gap is small, as assumed here, Equation (60) yields almost identical results as given by the formula based on cylindrical coordinates.

Recalling the definition in Equation (5)

$$L = \left(\frac{V_m\, g^2}{D} \right) y^*$$

and defining the flow rate per unit width by

$$q = V_m\, g \tag{61}$$

the percentage increase in saturation after a dimensionless length y^* is

$$S - S_e = \left(\frac{V_m\, g^2}{D} \right) y^* (DK)_w \left(\frac{P_{ii} - P_i}{T_i} + \frac{P_{oo} - P_o}{T_o} \right)$$

$$\frac{100}{9.1 \times 10^{-6} q} = 0.288\, gy^* \left(\frac{P_{ii} - P_i}{T_i} + \frac{P_{oo} - P_o}{T_o} \right) \% \tag{62}$$

In the above calculations $(DK)_w = 1.571 \times 10^{-11}$ $M/(\text{min.})\,(\text{cm.})\,(\text{mm. Hg})$ (*7*) and $D = 6.0 \times 10^{-4}$ sq.cm./min. (*12*) were used. The 9.1×10^{-6} represents the moles per liter of oxygen contained in fully saturated blood.

If a pressure difference of 640 mm. Hg is maintained across each membrane, Equation (62) becomes

$$S - S_e = 184\, gy^* \left(\frac{1}{T_i} + \frac{1}{T_o} \right) \% \tag{63}$$

For carbon dioxide removal, a mass balance equation may be written as

$$\kappa\, q \int_{P(0)}^{P(L)} \frac{dP}{P - P_w} = L(DK)_w \left(\frac{1}{T_i} + \frac{1}{T_o} \right) \tag{64}$$

in which κ is an assumed linearized proportionality between P_{CO_2} and total carbon dioxide content of the blood. Evaluating the integral, regrouping, and using 6.0×10^{-4} sq.cm./min. for carbon dioxide diffusivity in blood, 2.51×10^{-7} $M/(\text{ml.})\,(\text{mm. Hg})$ (*23*) for κ, and 8.33×10^{-11}

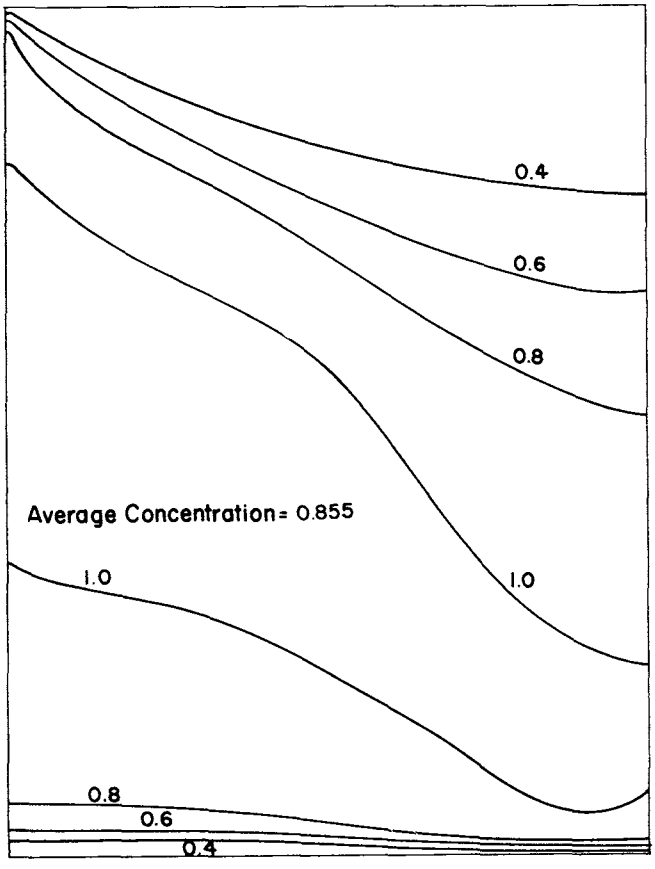

Fig. 14. Isoconcentration lines in meridian plane for perturbed laminar flow in curved channel exchanger. The exchage process is assumed to be fluid limited, and the wall concentration is zero. The cup-mixed average concentration is 0.855.

$M/(\text{min.})(\text{cm.})(\text{mm. Hg})$ for $(DK)_w$ (7)

$$\ln \frac{P(L) - P_w}{P(0) - P_w} = -0.553\, gy^* \left(\frac{1}{T_i} + \frac{1}{T_o}\right) \quad (65)$$

If $P(0) = 47$ mm. Hg and $P_w = 0$

$$P(y^*) = 47 \exp\left[-0.553\, gy^* \left(\frac{1}{T_i} + \frac{1}{T_o}\right)\right] \quad (66)$$

Equations (63) and (66) may be applied to calculate the dimensionless lengths necessary for the required saturation increase and carbon dioxide pressure drop. These lengths can then be compared with those obtained in the fluid-limited analysis to determine whether the oxygenator under consideration is fluid limited or wall limited.

ACKNOWLEDGMENT

The work reported in this paper was supported by the National Institutes of Health under Grants No. GM 00874 and GM 15418.

NOTATION

a = dimensionless critical wave number for disturbance
a_m = function as defined by Equation (28)
A = coefficient matrix for numerical scheme
A_m = expansion coefficient
b_m = function as defined by Equation (29)
B = constant vector in numerical scheme
B_m = expansion coefficient
C = gas concentration
C_m = function as defined by Equation (26)
$\frac{dp}{dy} = \frac{1}{r_m}\frac{\partial p}{\partial \varphi}$ = piezometric gradient along channel
D = gas diffusivity
$f(C)$ = oxygen or carbon dioxide sink characteristics in the blood
F = gas flux per unit length of the annulus
g = width between channel walls
h = coefficient
i = x^* coordinate index for finite-difference scheme
j = z^* coordinate index for finite-difference scheme
k = y^* coordinate index for finite-difference scheme
K = gas solubility
L = length of active exchange section
N = dimensionless parametric number
P = gas partial pressure
q = flow rate per unit width of channel
r = radial coordinate
S = percentage of hemoglobin saturated with oxygen
S_m = function as defined by Equation (27)
v = perturbation velocity
V = blood velocity
x = coordinate transverse to channel gap
y = coordinate along channel
z = coordinate along channel width

Greek Letters

α = amplitude factor for perturbation
β = constant scale factor for intensity of secondary circulations
γ = function as defined in Equation (25)
κ = assumed linearized proportionality between P_{CO_2} and total carbon dioxide content of the blood
λ_m = expansion coefficient
μ = absolute viscosity
μ_m = expansion coefficient
ν = kinematic viscosity
ξ = parameter defined in Equation (46)
ψ = dimensionless stream function

Subscripts

c = critical value
CO_2 = carbon dioxide
D = Dean
e = value at entrance to active section of channel exchanger
i = at outer surface of inner wall
ii = at inner surface of inner wall
m = mean value
o = at inner surface of outer wall
oo = at outer surface of outer wall
O_2 = oxygen
Re = Reynolds
w = value of variable at wall or value of wall parameter
x = component along x direction
y = component along y direction
z = component along z direction

Superscripts

* = dimensionless value
$'$ = derivative of function
$\bar{}$ = cup-mixed average

LITERATURE CITED

1. Brewster, D. B., P. Grosberg, and A. H. Nissan, *Proc. Roy. Soc. (London)*, **A251**, 76 (1959).
2. Buckles, R. B., E. W. Merrill, and E. R. Gilliland, *AIChE J.*, **14**, 703 (1968).
3. Chandrasekhar, S., "Hydrodynamic and Hydromagnetic Stability," Oxford Univ. Press (1961).
4. Chang, H. K., and L. F. Mockros, *AIChE J.*, **17**, No. 2, 397 (1971).
5. Dean, W. R., *Proc. Roy. Soc. (London)*, **A121**, 412 (1928).
6. Dorson, W. J., Jr., E. Baker, M. L. Cohen, B. Meyer, and M. Molthan, *Trans. Am. Soc. Artificial Internal Organs*, **15**, 155 (1969).
7. Dow Corning Corp., "Gas Transmission Rates of Plastic Films" (1959).
8. Drinker, P. A., R. H. Bartlett, R. M. Bailer, and B. S. Noyes, *Surgery*, **66**, 775 (1969).
9. Galletti, P. M., and G. A. Brecher, "Heart Lung Bypass," Grune and Stratton, New York (1962).
10. Gazley, C., *Trans. Am. Soc. Mech. Eng.*, **80**, 79 (1958).
11. Hammerlin, G., *Arch. Rational Mech. Analysis*, **1**, 212 (1958).
12. Keller, K. H., "Proceedings: Artificial Heart Program Conference," Natl. Heart Inst., Washington, D.C. (1969).
13. Pierce, E. C., II, *J. Mount Sanai Hospital*, **34** (5), 437 (1967).
14. Prins, J. A., J. Mulder, and J. Schenk, *Appl. Sci. Res.*, **A2**, 431 (1951).
15. Reid, W. H., *Proc. Roy. Soc. (London)*, **A244**, 186 (1958).
16. Richardson, L. F., and J. A. Gaunt, *Phil. Trans. Roy Soc. London*, **A226**, 299 (1927).
17. Robb, W. L., *General Electric Rept. No. 65-C-031* (1965).
18. Saul'yev, V. K., "Integration of Equations of Parabolic Type by the Methods of Nets," Pergamon Press, New York (1964).
19. Spaeth, E. E., and S. K. Friedlander, *Biophys. J.*, 7, 827 (1967).
20. Stuart, J. T., *J. Fluid Mech.*, **4**, 1 (1958).
21. Taylor, G. I., *Phil. Trans. Roy. Soc. London*, **A223**, 289 (1923).
22. Weissman, M. H., and T. K. Hung, *AIChE J.*, **17**, No. 1, 25 (1971).
23. Weissman, M. H., and L. F. Mockros, *J. Eng. Mech. Div., Am. Soc. Civil Eng.*, **93**, EM6, 225 (1967).
24. *Ibid.*, **94**, 857 (1968).

Manuscript received October 16, 1969; revision received February 23, 1970; paper accepted February 26, 1970.